The Fifteenth Korea-Japan Workshop on
Science and Technology in Ironmaking and Steelmaking
Okinawa, Japan, January 5 – 7, 2025

Modeling of Fluid Flow-Related Defects in Continuous Steel Casting

Seong-Mook Cho[1] and Brian G. Thomas[2]
[1] Department of Metallurgical Engineering,
Pukyong National University, Busan, Republic of Korea
[2] Department of Mechanical Engineering,
Colorado School of Mines, Golden, Colorado, USA
Corresponding authors: e-mail smcho1@pknu.ac.kr; bgthomas@mines.edu

Fluid flow phenomena greatly affect the quality of continuous cast steel. Air aspiration through a nozzle, due to negative pressure distribution, can cause reoxidation and non-metallic inclusions, which may build up on the refractory walls as nozzle clogging. Asymmetric jet flow from a clogged nozzle causes excessive surface velocities and vortexing at the top surface in the mold, resulting in entrainment of the mold slag into the steel pool. In addition, instability at the interface between the molten steel and surface slag, caused by jet wobbling, results in sudden level drops and slag entrapment into the solidifying shell at the meniscus region, leading to surface defects. Furthermore, particles such as argon gas bubbles, alumina inclusions and entrained slag droplets can be transported deep into the strand and captured into the steel shell. This causes internal defects. To quantify the above defect formation mechanisms related to fluid flow phenomena, high-resolution multiphase flow models validated with plant measurements and/or lab-scale model experiments are required.

Key words: steels; continuous casting; fluid flow; defects; computational models

1. Introduction

Many defects including both surface and internal defects on final steel products are associated with complex fluid-flow phenomena, including molten steel-argon gas flow, nozzle clogging, slag entrainment and entrapment, the transport of particles including non-metallic inclusions and argon gas bubbles, and particle capture into the solidifying steel shell during continuous casting (Fig. 1(a)).

Argon gas is injected into the molten steel to prevent the nozzle clogging. However, unoptimized injection conditions can produce undesirable mold flow, such as single-roll flow or unstable flow patterns which are detrimental to the top surface flow, level, and defect formation [1]. Alumina inclusions flow into the casting mold through the nozzle from upstream processes, such as steel making, ladle refining, and tundish operations [2]. In addition, air aspiration increases alumina inclusions due to reoxidation of the alloys melted in the molten steel, leading to the nozzle clogging [3]. A major cause of reoxidation is negative pressure inside the nozzle, which draws in air from the surroundings [3]. Clogging causes asymmetric internal shape of the nozzle bore and/or ports which can produce asymmetric flow in the mold during casting. This can lead to asymmetric and unstable flow across the top surface, causing excessive velocity, vortexing flow, and level fluctuations [4]. This in turn can lead to both slag entrainment into the molten steel pool [5,6] and the entrapment of inclusions during initial solidification, which is especially detrimental to the surface quality of steel [7].

Particles including argon gas bubbles, alumina inclusions, and entrained slag droplets can be transported to the steel shell front, where they may be captured into the solidifying shell [8].

Those captured particles become defects in the final cast steel, if the surface layer oxidized away by subsequent scale formation and scarfing processes are insufficient to remove them. Subsequent rolling operations elongate these captured particles in the casting direction. Captured bubbles may expand the surface during annealing processes and/or elongate during pressing, leading to blister defects on the surface of final steel products [2], such as shown in Fig. 1(b). Sliver defects due to the entrapment of alumina inclusions cause cracks and tearing during subsequent processes such as pressing, as shown in Fig. 1(c). Scab defects (Fig. 1(c)) associated with slag entrainment and entrapment appear with non-uniform shapes mostly on plate edge regions.

This paper briefly introduces various models to quantify the fluid flow phenomena related to defect formation in continuous steel casting. Then, defect formation mechanisms related to fluid flow are reviewed, such as air aspiration and nozzle clogging, surface level fluctuations leading to slag entrapment, alumina inclusion entrapment resulting in internal defects. Examples include fluid flow simulations validated with water model experiments and/or plant measurements.

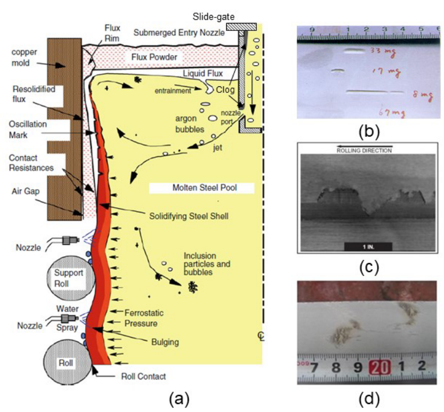

Fig. 1. (a) Schematic of various phenomena in a continuous casting mold [9], (b) blister [10], (c) sliver [10], (d) scab [11] defects in final steel products.

2. Models to Quantify Fluid Flow and Defects

To quantify fluid flow phenomena and the associated defects, computational modeling has been widely used, as reviewed previously [12-14]. Each model has both merits and limits. Thus, best is to apply various computational models validated with measurements in lab models and/or real plant.

Multiphase Computational Fluid Dynamics (CFD) models include Mixture and Eulerian-Eulerian (EE) models for molten steel-argon gas flow, Volume Of Fluid (VOF) for slag/steel interfacial motion, Lagrangian Discrete Phase Model (DPM) for particle trajectory, and the hybrid model, EEDPM for argon bubble interaction, particle capture models for particle entrapment between Primary Dendrite Arm Spacing (PDAS) and/or by subsurface hooks, as reviewed previously [12-14].

The developed computational models are validated via lab scale model experiments and/or plant measurements. Lab scale models using water or a low melting alloy is a useful tool, especially if similarity between the model and the real caster can be obtained. Matching both Froude number and Weber number is important to simulate multiphase flow phenomena, especially with high gas flow rates and volume fractions. This can be achieved with a 0.6 scale model [2, 15]. Plant measurements include nail dipping tests for surface velocity and level, and oscillation mark measurements for initial solidification, and surface profile variations. Particle capture measurements in as-cast slabs and billets include ultrasonic testing, step milling followed by visual or microscopy measurements and other methods reviewed previously [16]. Finally, it is important to observe and quantify the real defects found in the final products.

3. Air Aspiration and Nozzle Clogging

The pressure distribution inside the nozzle during continuous steel casting is important to steel quality. Fig. 2(a) shows the vertical pressure distribution inside a nozzle with a slide gate, predicted from both a three-dimensional EE model simulation of molten steel-argon gas flow with FLUENT [17] and a one-dimensional pressure-energy model calculation using the Pressure-drop Flow-rate model for Slide Gate systems program (PFSG) [18]. Both model predictions match reasonably and reveal a large negative pressure region from the middle plate to the meniscus. The negative pressure is generated by sudden contraction of the nozzle bore due to the reduced area of the slide-gate opening, which controls molten steel flow rate during continuous casting. The negative pressure region indicates possible air aspiration region, resulting in reoxidation and oxide inclusions. Buildup of these inclusions on the nozzle walls often lead to nozzle clogging, shown in Fig. 2(b), especially in regions such as near the slide gate and/or the upper region of nozzle ports, where the flow is relatively stagnant due to recirculation.

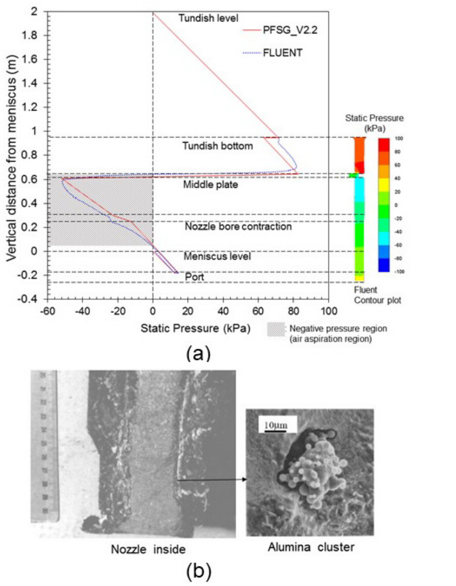

Fig. 2 (a) Pressure distribution [19] and (b) clogging inside a nozzle [20,21].

4. Slag/Steel Interface Fluctuations and Surface Defects

The jets from nozzle ports generate flow patterns and liquid mold flux behavior in the mold, as shown for example in Fig. 3(a). As shown in Fig. 3(a), a finger-like protrusion from the liquid slag layer is observed near where the jet impinges on the top surface. Jet wobbling due to an unstable flow pattern associated with the upward nozzle port (Fig. 3(a)) produces transient variations in the impingement point on the top surface, leading to this entrainment phenomenon [11]. Flow variations inside the nozzle are another way that jet wobbling, velocity variations, level fluctuations, and defects can occur.

Slag entrained near the meniscus can be directly entrapped into the initial solidification front. Fig. 3(b) shows an instantaneous surface slag/molten steel interface predicted from the LES-VOF simulation shown in Fig. 3(a) and potential slag entrainment regions near the meniscus. The surface level drops over 10 mm relative to the time-average level, which can produce an 8 mm vertical-length of slag entrainment. Such entrapped slag can become a surface defect if the slag is unable to be removed during scale formation or subsequent scarfing processes (Fig. 3(c)).

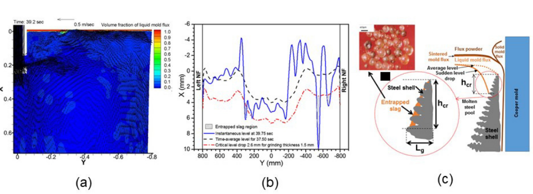

Fig. 3 (a) Instantaneous jet flow impinging on top surface, (b) sudden surface-level drops causing slag entrapment, and (c) schematic of the slag entrapment mechanism [11].

5. Particle Capture into Solidifying Steel Shell and Internal Defects

Particles delivered deep into the strand can be detrimental to internal steel quality if they are entrapped by the solidifying steel shell: either by entering between the primary dendrite arms, or by balancing at the front while they become surrounded by the growing dendrites. These particles become internal defects.

Fig. 4 shows the flow patterns and the argon-bubble capture locations in a typical strand caster that has a curved region starting a below and upper straight region that includes the mold. A large recirculation region (over 2 m long) with flow stagnation is generated near the straight/curved transition region, as shown in the side views taken at the quarter vertical plane (0.58 m from the strand center). This flow recirculation is likely due to bubble buoyancy causing rising flow in the relatively stagnant region near the inside radius shell. Strong downward flow from the jets impinging on the narrow faces tends to extend straight down near the outside radius shell. More particles are captured at the stagnant or upward flowing regions: the straight/curved transition on IR or deeper in the strand.

Finally, the entrapped particles remain in the solidified steel slab, as shown in end view of the strand (Fig. 4(c), note: the colored dots (predicted from the particle capture simulation) and the black dots (measured from the UT measurements) show the locations of captured particles). Most captured particles are observed near the straight/curved transition region (green dash line), as also shown in Fig. 4(b). These particles are detrimental to the quality of final steel products after later processing. Especially, the captured bubbles expand during annealing process, and then elongate during pressing process, resulting in pencil pipe blister defects on the final steel product.

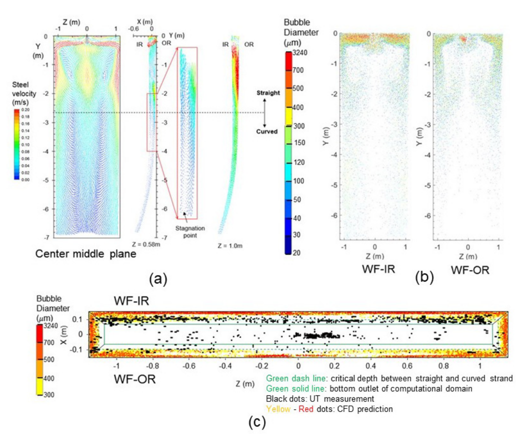

Fig. 4 (a) Fluid flow patterns and (b) alumina inclusion capture distributions on wide faces and (c) in end view of steel slab in strand casting [19].

6. Summary and Conclusions

This paper provides examples of fluid flow-related defects in continuous steel casting, quantified by applying various multiphase CFD models. Some important conclusions are summarized below:

- High-resolution multiphase flow modeling validated with measurements using water models and/or a real plant is best to accurately quantify the mechanisms of fluid flow-related defect formation.
- Air aspirated into the nozzle due to negative pressure produces non-metallic inclusions, leading to buildup of the inclusions on the nozzle walls and nozzle clogging. This can cause asymmetric mold flow and vortex formation, and excessive surface velocity and level fluctuations, leading to slag entrainment defects.
- Surface level fluctuations can cause both slag entrainment and particle entrapment near the meniscus region, leading to surface defects.
- Particles delivered deep into the strand can be captured between the primary dendrite arms or surrounded by the growing dendrites, leading to internal defects. The inside radius near the straight/curved transition of the caster is more prone to capture large particles, because a flow recirculation region is generated there.

Acknowledgements

Support from the Continuous Casting Center at Colorado School of Mines, the Continuous Casting Consortium at University of Illinois at Urbana-Champaign, POSCO, South Korea (Grant No. 4.0011721.01), and the National Science Foundation GOALI grant (Grant No. CMMI 18-08731) are gratefully acknowledged. Provision of FLUENT licenses through the ANSYS Inc. academic partnership program is also much appreciated. This research is part of the Blue Waters sustained-petascale computing project, which is supported by the National Science Foundation (awards OCI-0725070 and ACI-1238993) and the state of Illinois. Blue Waters is a joint effort of the University of Illinois at Urbana-Champaign and its National Center for Supercomputing Applications. Thanks are also given to Mingyi Liang, Hamed Olia, and Lipsa Das.

References

1. P. H. Dauby: Revue de Métallurgie, 109 (2012), 113.
2. L. Zhang, S. Yang, K. Cai, J. Li, X. Wan, B. G. Thomas: Metall. Mater. Trans. B, 38 (2007), 63.
3. K. Rackers, B. G. Thomas: The 78th Steelmaking Conference, Nashiville, TN., USA., 2 April 1995.
4. S.-M. Cho, S.-H. Kim, R. Chaudhary, B. G. Thomas, H.-J. Shin, W.-Y. Choi, S.-K. Kim: Iron Steel Technol. 9 (2012), 85.
5. S.-M. Cho, B. G. Thomas, S-H. Kim, H.-J. Lee: CCC Annual Meeting, Champaign, IL., USA., 19 August 2015.
6. L. C. Hibbeler, B. G. Thomas: Iron Steel Technol., 10 (2013), 121.
7. H.-J. Shin, S.-H. Kim, B. G. Thomas, G.-G. Lee, J.-M. Park, J. Sengupta: ISIJ Int., 46 (2016), 1635.
8. B. G. Thomas, Q. Yuan, S. Mahmood, R. Liu, R. Chaudhary: Metall. Mater. Trans. B, 45 (2014), 22.
9. B. G. Thomas: ccc.Illinois.edu.
10. G.-G. Lee, B. G. Thomas: CCC Annual Meeting, Champaign, IL., USA., 12 June 2007.
11. S.-M. Cho, B. G. Thomas, S.-H. Kim: Metall. Mater. Trans. B, 50 (2019), 52.
12. S.-M. Cho, B. G. Thomas: Metals, 9 (2019), 471.
13. H. Yang, S. P. Vanka, B. G. Thomas: ISIJ Int., 56 (2019), 956.
14. B. G. Thomas: Steel Res. Int., 89 (2018), 1700312.
15. P. K. Singh, D. Mazumdar: Metall. Mater. Trans. B, 50 (2019), 1091.
16. L. Zhang, B. G. Thomas: ISIJ Int., 43 (2003), 271.
17. ANSYS FLUENT 14.5-Theory Guide, ANSYS. Inc., Canonsburg, PA., USA, 2012.
18. H. Olia, H. Yang, S.-M. Cho, M. Liang, L. Das, B. G. Thomas: Metall. Mater. Trans. B, 53 (2022), 1661.
19. M. Liang, S.-M. Cho, H. Olia, L. Das, B. G. Thomas: AISTECH 2019, Pittsburgh, PA., USA., 6-9 May 2019.
20. K. G. Rackers: M.S. Thesis, Univ. of Illinois, 1995.
21. R. A. Rege, E. S. Szekeres, W. D. Forgeng: Met. Trans. AIME, 1 (1970), 2652.

Reprinted from
"Multiphase Flow-Related Defects in Continuous Casting of Steel Slabs" S-M. Cho, M. Liang, H. Olia, L. Das, and B. G. Thomas; TMS 2020 149th Annual Meeting & Exhibition Supplemental Proceedings, 1161-1173, (2020).